Long-wavelength quantum and classical plasma frequencies in fractional-dimensional space

2008 J. Phys.: Condens. Matter 20 485201

(http://iopscience.iop.org/0953-8984/20/48/485201)

J. Phys.: Condens. Matter **20** (2008) 485201 (8pp) doi:10.1088/0953-8984/20/48/485201

Long-wavelength quantum and classical plasma frequencies in fractional-dimensional space

S Panda[1] **and B K Panda**[2]

[1] Institute of Mathematics and Applications, Surya Kiran Building, Saheed Nagar, Bhubaneswar, India
[2] Plot-297, Behera Sahi, Bhubaneswar 751007, Orissa, India

Received 6 August 2008
Published 17 October 2008
Online at stacks.iop.org/JPhysCM/20/485201

Abstract
Long-wavelength plasma frequencies have been obtained in the modified random phase approximation (RPA) and plasmon-pole approximation (PPA) methods for both quantum and classical plasmas in fractional-dimensional space. The dynamical local-field factor is included in the dielectric function. Comparison of the plasma frequencies in these methods shows that both RPA and PPA methods are quite accurate in finding plasma frequencies. Although the contribution of the dynamical local-field factor to the quantum plasma frequency is quite significant, it vanishes for the classical plasma. While the quantum plasma is undamped in the collective excitation regime, the classical plasma is damped in this regime.

1. Introduction

In a quantum well (QW) with infinitely large barrier widths, the electron and hole wavefunctions are confined in the well region. In view of the spatial extension of the excitons [1] and polarons [2], the QW shows two-dimensional (2D) behavior when the well width is extremely narrow. The dimension of the system increases with increasing well width. At large well width the system shows three-dimensional (3D) behavior. The QW with infinite barrier heights and finite well width shows fractional-dimensional (FD) behavior with the dimension α lying somewhere between 2 and 3.

The situation in a QW with finite confining potential is different. In this well the energy level approaches the edge of the well, so that effectively the particles are spread over the barrier region. When the well width is extremely small, the wavefunctions are mainly confined in the barrier region so that the system shows 3D characteristics of the barrier materials. In a QW well with large well width, the electron and hole wavefunctions are mostly confined in the well region so that the system shows 3D behavior of the well material. This behavior has been established in the properties of exciton [3] and polaron [4, 5] in a QW. Consequently, the system shows FD characteristics when the well width is in the range 10–100 Å.

The real confining structure in the FD space is replaced by an isotropic space where the measure of its anisotropy or confinement is given by the fractional dimension α [6]. Such a space, termed as *dynamic space*, differs from the geometric space in that its dimensionality is determined by physical interactions, as seen from the viewpoint of excitation dynamics. The FD space is not in general a vector space and the coordinates in this space are termed as *pseudocoordinates*. This approach has been applied to study exciton [7–9] and absorption spectra in QWs and quantum wires [10]. It has also been applied to study the biexcitons [11–13], the exciton–phonon interactions [14], the Stark shift of excitonic complexes [15], the refractive index [16], the impurity states [17], the Pauli blocking effect [18], the polaron effect in QWs [19, 20] and the exciton–polaron properties in QWs [21]. The calculation of the ground state properties of excitons has been carried out in the undoped system where the electron–hole interaction is not screened by the electron and hole carrier densities. The screening in 3D [22] and 2D [23] systems has been carried out by the dielectric functions. Similarly the many-polaron system in the degenerate system requires the electron–phonon interaction to be screened by the electron density [24]. Unfortunately the dielectric function is not known in an FD space.

The dielectric functions are calculated in the linear response theory [25–28]. In the direct method a monochrome perturbation is added to the external potential and the perturbed charge density is obtained with the new external potential [29]. The change in charge density is obtained by comparing it

with the unperturbed charge density. The dielectric function is related to the ratio of the change in charge density with the change in external potential. This procedure is quite involved and it has the limitation that it can only be used to calculate the dielectric function in the static limit. On the other hand the calculation of the dielectric function in the random phase approximation (RPA) method is simple. Since it is based on the time-dependent Hartree equation, the frequency dependence is included in the dielectric function. The roots of the dielectric function give plasma frequencies. Although it is not an exact theory, it is still accurate at zero temperature when the electron density is high in the medium [30]. The RPA becomes a progressively better approximation when the temperature increases. At high temperature it works well irrespective of the magnitude of electron density in the material [30]. In the long-wavelength limit the plasmon frequency is obtained in a closed form. The accuracy of the plasma frequencies at finite wavevector calculated numerically in the RPA method can be checked by comparing them with the analytic frequencies in the long-wavelength limit.

The plasmon-pole approximation (PPA) technique is another simplification of the RPA method for determining the long-wavelength plasma frequencies [27, 31–33]. The wavevector dependence in plasma frequency is obtained from the sum rules [26]. The Fröhlich interaction involving the electron scattering by phonon, plasmon and plasmon–phonon hybrid modes is based on the PPA method and the interaction strength is significant in the long-wavelength limit. The ground state properties of the plasma–polaron strength [34], the electron transport in semiconductors [35] and the electron self-energy [30, 36] have been studied using this method. Therefore it is important to find plasma frequencies using this method.

Depending upon the temperature of the system, the plasma is classified as either quantum or classical plasma. When the temperature of the system is well below the Fermi temperature ($T_{\rm F}$), the Fermi–Dirac statistical distribution function is usually employed and the plasma is termed as a quantum plasma. Using the RPA method, the plasma dispersion has been studied in 3D [37], 2D [38] and 1D [30] quantum plasmas at zero temperature. The plasma frequencies at finite temperature have been calculated in 3D [39], 2D [39, 40] and 1D [30] systems and these are found to increase with temperature. In 3D systems, the plasmon decays into electron–hole pairs when it enters into the electron–hole continuum at the plasmon critical wavevector q_c. In 2D systems, the plasmon ceases to exist beyond $q_{\rm c}$. Since there is no $q_{\rm c}$ in 1D systems, the plasmon does not decay into the electron–hole pair.

The quantum plasma shows quantum interference due to the long de Broglie wavelength of particles and this introduces higher-order many-body effects which give rise to a dynamical local-field factor (LFF) [26]. As a result of this the Coulomb potential is reduced and the reduction in Coulomb potential reduces the plasma frequencies in comparison with those obtained in the RPA method. Using different techniques, the plasma frequencies have been studied in the 3D [36, 41, 42], 2D [43, 44] and 1D [45, 46] systems.

When the temperature of the system is well above $T_{\rm F}$, the distribution function changes from Fermi–Dirac to Maxwell–Boltzmann type and this results in a classical plasma. Since at high temperature the RPA method works well for both low and high electron density of the system, the dispersion of classical plasma frequencies has been evaluated using this method. The wavevector dependence of the classical plasma and the damping of the plasma frequency have been studied in 3D [25, 47, 48] and 2D [49–53] systems.

In the present work, the quantum and classical plasma frequencies have been calculated using both the modified RPA and PPA methods in the FD space. The simplest static LFF by Hubbard is not taken into account as it is an approximate method of calculating LFF due to the exchange effect [54]. Since the plasma frequency manifests a dynamical property, the dynamical LFF needs to be included in the dielectric function for evaluating it. In section 2 we outline the methods for evaluating plasma frequency and damping. In sections 3 and 4 we apply these methods to quantum plasma at zero- and finite-temperature limits, respectively. In section 5, the frequency and damping of classical plasma are discussed. Finally the paper is concluded in section 6.

2. Method of calculation

The modified dielectric function which includes dynamical LFF is defined as [25, 28]

$$\epsilon_{\alpha D}(q,\omega;\mu,T) = \epsilon_b\left[1-\frac{Q^{(0)}_{\alpha D}(q,\omega;\mu,T)}{1+G_{\alpha D}(q,\omega;\mu,T)Q^{(0)}_{\alpha D}(q,\omega;\mu,T)}\right], \quad (1)$$

where ϵ_b is the bulk dielectric constant, μ is the chemical potential, $G_{\alpha D}(q,\omega;\mu,T)$ is the dynamical LFF at temperature T and the Lindhard function $Q^{(0)}_{\alpha D}(q,\omega;\mu,T)$ is defined as

$$Q^{(0)}_{\alpha D}(q,\omega;\mu,T) = v_{\alpha D}(q)\chi^{(0)}_{\alpha D}(q,\omega;\mu,T). \quad (2)$$

Here, $v_{\alpha D}(q)$ is the Fourier transform of the Coulomb potential and $\chi^{(0)}_{\alpha D}(q,\omega;\mu,T)$ is the temperature-dependent irreducible polarizability function. For the long-range interaction $1/r$, $v_{\alpha D}(q)$ has been derived as [20]

$$v_{\alpha D}(q) = \frac{(4\pi)^{\frac{\alpha-1}{2}}\Gamma\left(\frac{\alpha-1}{2}\right)e^2}{\epsilon_b q^{\alpha-1}}, \quad (3)$$

where $\Gamma(x)$ is the Euler-gamma function [55]. Since $\Gamma(0)$ diverges, $v_{\alpha D}(q)$ cannot be defined for 1D systems. Such a potential corresponds to a system embedded in 3D space such as QW and quantum wire. In a strictly 2D system the Coulomb potential is assumed to be in the $\log r$ form [56, 57]. The plasmon frequency in a strictly 2D system has a gap at $q = 0$. In a strictly lower-dimensional system ($1 < \alpha < 2$) the Fourier transform of the potential is of the form $g_{\rm c}/q^{2\alpha-2}$, where $g_{\rm c}$ is the coupling constant [57, 58]. This potential predicts the plasma frequency gapless at $q = 0$. In the present work we have chosen the long-range $1/r$ Coulomb potential for calculating plasma frequencies which is appropriate for confined systems.

The non-interacting polarizability function in FD space is defined as [25, 28]

$$\chi^{(0)}_{\alpha D}(q,\omega;\mu,T) = \frac{2}{V_{\alpha D}}\sum_{\mathbf{k}}\frac{n_{\mathrm{F}}(\mathbf{k}) - n_{\mathrm{F}}(\mathbf{k}+\mathbf{q})}{E_{\mathbf{k}} - E_{\mathbf{k}+\mathbf{q}} + \hbar\omega + \mathrm{i}\delta}, \quad (4)$$

where $n_{\mathrm{F}}(\mathbf{k})$ is the Fermi–Dirac distribution function at temperature T, the band energy $E_k = \hbar^2k^2/2m^*$ with m^* being the electron effective mass, $V_{\alpha D}$ is the volume in FD space and $\delta = 0^+$. In the FD space, the summation over $\mathbf{k}$ is converted to an integral as [6]

$$\sum_{\mathbf{k}}\cdots = \frac{V_{\alpha D}}{(2\pi)^\alpha}\frac{2\pi^{\frac{\alpha-1}{2}}}{\Gamma(\frac{\alpha-1}{2})}\int_0^\infty\int_0^\pi k^{\alpha-1}\,\mathrm{d}k\,\sin^{\alpha-2}\theta\,\mathrm{d}\theta\cdots. \quad (5)$$

This transformation is not valid for 1D systems as $\Gamma(0)$ diverges when $\alpha = 1$. Using equation (5) in (4) and carrying out the θ integration, the real part $Q^{(0)}$ in the long-wavelength limit is derived as

$$\mathrm{Re}[Q^{(0)}_{\alpha D}(q,\omega;\mu,T)] = \frac{2e^2q^{3-\alpha}\Gamma\left(\frac{\alpha-1}{2}\right)}{\sqrt{\pi}\epsilon_b m^*\Gamma(\frac{\alpha}{2})}\frac{1}{\omega^2} \times\left[\int_0^\infty n_{\mathrm{F}}(\mathbf{k})k^{\alpha-1}\,\mathrm{d}k + \frac{3\hbar^2q^2}{\alpha m^{*2}\omega^2}\int_0^\infty n_{\mathrm{F}}(\mathbf{k})k^{\alpha+1}\,\mathrm{d}k\right]. \quad (6)$$

The imaginary part in the long-wavelength limit after θ integration is obtained as

$$\mathrm{Im}[Q^{(0)}_{\alpha D}(q,\omega;\mu,T)] = -\frac{2m^*e^2}{\epsilon_b\hbar^2q^\alpha} \times\left[\int_{k_+}^\infty n_{\mathrm{F}}(\mathbf{k})(k^2-k_+^2)^{\frac{\alpha-3}{2}}k\,\mathrm{d}k - \int_{k_-}^\infty n_{\mathrm{F}}(\mathbf{k})(k^2-k_-^2)^{\frac{\alpha-3}{2}}k\,\mathrm{d}k\right], \quad (7)$$

where $k_\pm$ is defined as

$$k_\pm = \frac{m^*}{\hbar^2q}(\hbar\omega \pm E_q). \quad (8)$$

The dynamical LFF is calculated using the first-order exchange and self-energy contributions to the irreducible polarization [43, 44]. It is qualitatively similar to the time-dependent Hartree–Fock (HF) method. In this method the dynamical LFF is defined as

$$G_{\alpha D}(q,\omega;\mu,T) = \{Q^{(1)}_{\alpha D}(q,\omega;\mu,T)\}\{Q^{(0)}_{\alpha D}(q,\omega;\mu,T) \times[Q^{(0)}_{\alpha D}(q,\omega;\mu,T) - Q^{(1)}_{\alpha D}(q,\omega;\mu,T)]\}^{-1} \quad (9)$$

where the contribution of the first-order exchange and self-energy diagrams at large ω is given by

$$Q^{(1)}_{\alpha D}(q,\omega;\mu,T) = \frac{\omega^4_{\alpha D}(q)}{\omega^4}G^{\mathrm{HF}}_{\alpha D}(q;\mu,T) + \mathrm{O}\left(\frac{1}{\omega^6}\right) \quad (10)$$

where $G^{\mathrm{HF}}_{\alpha D}(q;\mu,T)$ is the static LFF in the HF theory. It is given as

$$G^{\mathrm{HF}}_{\alpha D}(q;\mu,T) = \frac{1}{n_{\alpha D}q^{\alpha+1}}\int\frac{\mathrm{d}^\alpha k}{(2\pi)^\alpha}\frac{(\mathbf{q}\cdot\mathbf{k})^2}{k^{\alpha-1}} \times[S^{\mathrm{HF}}_{\alpha D}(\mathbf{k};\mu,T) - S^{\mathrm{HF}}_{\alpha D}(\mathbf{k}+\mathbf{q};\mu,T)]. \quad (11)$$

The HF structure factor $S^{\mathrm{HF}}_{\alpha D}(k,T)$ is defined as

$$S^{\mathrm{HF}}_{\alpha D}(\mathbf{k};\mu,T) = -\frac{\hbar}{\pi n_{\alpha D}v_{\alpha D}(q)} \times\int_0^\infty \mathrm{d}\omega\coth\left(\frac{\hbar\omega}{2k_{\mathrm{B}}T}\right)\mathrm{Im}\,Q^{(0)}_{\alpha D}(\mathbf{k},\omega;\mu,T). \quad (12)$$

On simplification, we find

$$G^{\mathrm{HF}}_{\alpha D}(q;\mu,T) = \frac{(7-\alpha)}{4(\alpha+2)k_\mu}\left(\frac{q}{k_\mu}\right)^{\alpha-1} \times\int_0^\infty \mathrm{d}k[1 - S^{\mathrm{HF}}_{\alpha D}(\mathbf{k};\mu,T)] \quad (13)$$

where $k_\mu = \sqrt{2m^*\mu/\hbar^2}$ with μ being the chemical potential. At zero temperature $\mu = E_{\mathrm{F}}$ and $k_\mu = k_{\mathrm{F}}$.

In the RPA method the plasma frequencies are obtained from the roots of $\epsilon_{\alpha D}(q,\omega;\mu,T) = 0$. Since the plasma frequencies are Landau damped [59], the frequencies are in general complex, $\omega = \Omega_{\alpha D}(q,T) - \mathrm{i}\gamma_{\alpha D}(q,T)$, where $\Omega_{\alpha D}(q,T)$ and $\gamma_{\alpha D}(q,T)$ are the plasma frequency and collisionless plasma damping, respectively. For small $\gamma_{\alpha D}(q)$, the real part of equation (1) gives the condition [25]

$$1 - \mathrm{Re}[Q^{(0)}_{\alpha D}(q,\Omega(q,T);\mu,T)] + \mathrm{Re}[Q^{(1)}_{\alpha D}(q,\Omega_{\alpha D}(q,T);\mu,T)] = 0. \quad (14)$$

The roots of this equation give $\Omega_{\alpha D}(q,T)$. The imaginary part gives the collisionless plasma damping

$$\gamma_{\alpha D}(q,T) = \mathrm{Im}[Q^{(0)}_{\alpha D}(q,\Omega_{\alpha D}(q,T);\mu,T)] \times\left[\frac{\partial\,\mathrm{Re}[Q^{(0)}_{\alpha D}(q,\omega;\mu,T)]}{\partial\omega}\bigg|_{\Omega_{\alpha D}(q,T)}\right]^{-1}. \quad (15)$$

The plasmon-pole approximation (PPA) method gives a simple form for the plasmon frequency $\Omega^{(p)}_{\alpha D}(q,T)$ as [32]

$$\Omega^{(p)}_{\alpha D}(q,T) = \omega_{\alpha D}(q)\left[\frac{\epsilon_{\alpha D}(q,0,T)}{\epsilon_{\alpha D}(q,0,T) - \epsilon_b}\right]^{\frac{1}{2}}. \quad (16)$$

The evaluation of plasma frequency needs the dielectric function containing a static LFF. In the present case we have used the static LFF in the HF model described in equation (13). Although the PPA method is successful in finding the plasmon frequencies, the plasma damping cannot be calculated using this method.

3. Long-wavelength plasma frequency in the quantum plasma at zero temperature

We consider the zero-temperature limit $n_{\mathrm{F}}(\mathbf{k}) = \theta(k_{\mathrm{F}} - k)$, where k_{F} is the Fermi momentum. The expression for k_{F} in FD space has been given as [58]

$$k_{\mathrm{F}} = \left(\frac{(4\pi)^{\frac{\alpha}{2}}\Gamma(1+\frac{\alpha}{2})n_{\alpha D}}{2}\right)^{\frac{1}{\alpha}}. \quad (17)$$

It is easy to carry out the integration over k in equation (4). The expression for the real part of $Q^{(0)}(q,\omega,0)$ is obtained as

$$\mathrm{Re}[Q^{(0)}_{\alpha D}(q,\omega,E_\mathrm{F},0)] = \frac{\omega^2_{\alpha D}(q)}{\omega^2}\left[1+\frac{3q^2v_\mathrm{F}^2}{(\alpha+2)\omega^2}\right] + \mathrm{O}\left(\frac{1}{\omega^6}\right), \tag{18}$$

where the Fermi velocity $v_\mathrm{F} = \hbar k_\mathrm{F}/m^*$ and $\omega_{\alpha D}(q)$ is obtained as

$$\omega_{\alpha D}(q) = \sqrt{\frac{(4\pi)^{\frac{\alpha-1}{2}}\Gamma(\frac{\alpha-1}{2})e^2 n_{\alpha D}q^{3-\alpha}}{\epsilon_b m^*}}. \tag{19}$$

Here, $\omega_{\alpha D}(q) \propto q^{(3-\alpha)/2}$. Therefore, it is independent of q for $\alpha = 3$. For $\alpha < 3$, it vanishes at $q = 0$.

The first-order contribution can be obtained by evaluating $Q^{(1)}_{\alpha D}(q,\omega,E_\mathrm{F},0)$. The imaginary part of the polarizability function at $T = 0$ is derived by carrying out the integration over k in equation (7):

$$\mathrm{Im}[Q^{(0)}_{\alpha D}(q,\omega,E_\mathrm{F},0)] = \frac{2m^*}{(\alpha-1)\epsilon_b\hbar^2q^\alpha}[\Theta(k_\mathrm{F}-k_+)(k_\mathrm{F}^2-k_+^2)^{\frac{\alpha-1}{2}} - \Theta(k_\mathrm{F}-k_-)(k_\mathrm{F}^2-k_-^2)^{\frac{\alpha-1}{2}}]. \tag{20}$$

Thus, $S^{\mathrm{HF}}_{\alpha D}(q,E_\mathrm{F},0)$ can be derived as

$$S^{\mathrm{HF}}_{\alpha D}(q,E_\mathrm{F},0) = \frac{\alpha\Gamma(\frac{\alpha}{2})q}{(\alpha-1)\Gamma(\frac{\alpha-1}{2})\sqrt{\pi}k_\mathrm{F}} \times {}_2F_1\left(\frac{1}{2},\frac{1-\alpha}{2};\frac{3}{2};\frac{q^2}{4k_\mathrm{F}^2}\right), \tag{21}$$

where ${}_2F_1$ is the hypergeometric function [56]. Using equation (21) in (13), $G^{\mathrm{HF}}_{\alpha D}$ is obtained as

$$G^{\mathrm{HF}}_{\alpha D}(q,E_\mathrm{F},0) = \frac{\alpha(7-\alpha)}{4(\alpha+2)}\frac{\Gamma(\frac{\alpha}{2})}{\pi^{\frac{1}{2}}\Gamma(\frac{3+\alpha}{2})}\left(\frac{q}{k_\mathrm{F}}\right)^{\alpha-1}. \tag{22}$$

Taking $Q^{(0)}_{\alpha D}$ and $Q^{(1)}_{\alpha D}$ in equation (14), the plasma frequency is obtained as

$$\Omega_{\alpha D}(q,0) = \omega_{\alpha D}(q) + \frac{q^2v_\mathrm{F}^2}{\omega_{\alpha D}(q)} \times \left[\frac{3}{2(\alpha+2)} - \frac{(7-\alpha)\Gamma(\frac{\alpha}{2})}{8(\alpha+2)\pi^{\frac{1}{2}}\Gamma(\frac{\alpha+3}{2})}\left(\frac{q_{\mathrm{TF}}(0)}{k_\mathrm{F}}\right)^{\alpha-1}\right] \tag{23}$$

where q_{TF} is the Thomas–Fermi wavevector at $T = 0$. It is defined as $q_{\mathrm{TF}}^{\alpha-1}(0) = v_{\alpha D}(q)q^{\alpha-1}\frac{\partial n_{\alpha D}}{\partial E_\mathrm{F}}$, where E_F is the Fermi energy. Using equation (17), $q_{\mathrm{TF}}(0)$ is derived as

$$q_{\mathrm{TF}}^{\alpha-1}(0) = \frac{\alpha\omega^2_{\alpha D}(q)q^{\alpha-3}}{v_\mathrm{F}^2}. \tag{24}$$

The plasmon frequency can be calculated in the PPA method by using equation (16). In the compressibility sum rule, $\epsilon_{\alpha D}(q,0,0)$ including the HLFF is given as [26]

$$\lim_{q\to0}\epsilon_{\alpha D}(q,0;E_\mathrm{F},0) = \epsilon_b\left(1+\frac{(q_{\mathrm{TF}}(0)/q)^{\alpha-1}}{1-G^{\mathrm{HF}}_{\alpha D}(q;E_\mathrm{F},0)(q_{\mathrm{TF}}(0)/q)^{\alpha-1}}\right). \tag{25}$$

The plasmon frequency in the long-wavelength limit in the PPA method is then found as

$$\Omega^{(p)}_{\alpha D}(q,0) = \omega_{\alpha D}(q) + \frac{q^2v_\mathrm{F}^2}{\omega_{\alpha D}(q)} \times \left[\frac{1}{2\alpha} - \frac{(7-\alpha)\Gamma(\frac{\alpha}{2})}{8(\alpha+2)\pi^{\frac{1}{2}}\Gamma(\frac{\alpha+3}{2})}\left(\frac{q_{\mathrm{TF}}(0)}{k_\mathrm{F}}\right)^{\alpha-1}\right]. \tag{26}$$

The contribution of leading and LFF terms to the plasma frequency in equation (26) is the same as in equation (23). The plasma frequencies are calculated taking $m^* = 0.067m_0$ and $\epsilon_b = 1$. In figure 1 the scaled plasma frequency, $W_{\alpha D}(q,0) = \Omega_{\alpha D}(q,0)/w_{\alpha D}$ where the Fermi frequency $w_{\alpha D} = E_\mathrm{F}/\hbar$, is shown as a function of the scaled wavevector q/k_F for several values of r_s. Both the methods give similar results for all r_s values. The slight discrepancy arises due to static LFF used in the PPA method. The quantum plasma shows quantum interference due to long de Broglie wavelength of particles. The quantum interference produces higher-order many-body effects.

The plasma oscillations at zero temperature do not decay in the long-wavelength limit since $\mathrm{Im}[Q^{(0)}(q,\Omega_{\alpha D}(q,0);E_\mathrm{F},0)] = 0$.

4. Long-wavelength plasma frequency in the quantum plasma at finite temperature

We follow the method of Cetina *et al* [60] to carry out the integrals in equation (6) for $T \leqslant T_\mathrm{F}$ to find $Q^{(0)}(q,\omega,T)$. After carrying out the straightforward algebra we find

$$\mathrm{Re}[Q^{(0)}_{\alpha D}(q,\omega;\mu,T)] = \frac{\omega^2_{\alpha D}(q,T)}{\omega^2}\left[1+\frac{3q^2v_\mu^2}{(\alpha+2)\omega^2} \times \left\{1+\frac{5\alpha(\alpha+2)\pi^2}{24}\left(\frac{k_\mathrm{B}T}{\mu}\right)^2+\mathrm{O}\left(\frac{k_\mathrm{B}^4T^4}{\mu^4}\right)\right\}\right] + \mathrm{O}\left(\frac{1}{\omega^6}\right) \tag{27}$$

where $v_\mu = \hbar k_\mu/m^*$ and the temperature-dependent density $n_{\alpha D}(T)$ is given by

$$n_{\alpha D}(T) = \left(\frac{2m^*}{\hbar^2}\right)^{\frac{\alpha}{2}}\frac{\mu^{\frac{\alpha}{2}}}{\alpha 2^{\alpha-2}\pi^{\frac{\alpha}{2}}\Gamma(\frac{\alpha}{2})} \times \left[1+\alpha(\alpha+2)\frac{\pi^2}{24}\left(\frac{k_\mathrm{B}T}{\mu}\right)^2+\mathrm{O}\left(\frac{k_\mathrm{B}^4T^4}{\mu^4}\right)\right]. \tag{28}$$

For $\alpha = 2$ and $T < T_\mathrm{F}$, μ has been derived as [60]

$$\mu = E_\mathrm{F}\left\{1+\left(\frac{k_\mathrm{B}T}{E_\mathrm{F}}\right)\log\left[1-\exp\left(-\frac{E_\mathrm{F}}{k_\mathrm{B}T}\right)\right]\right\}. \tag{29}$$

For $\alpha \neq 2$, the expression for μ has been given as [60]

$$\mu = E_\mathrm{F}\left[1-\frac{\pi^2}{12}(\alpha-2)\left(\frac{k_\mathrm{B}T}{E_\mathrm{F}}\right)^2\right]. \tag{30}$$

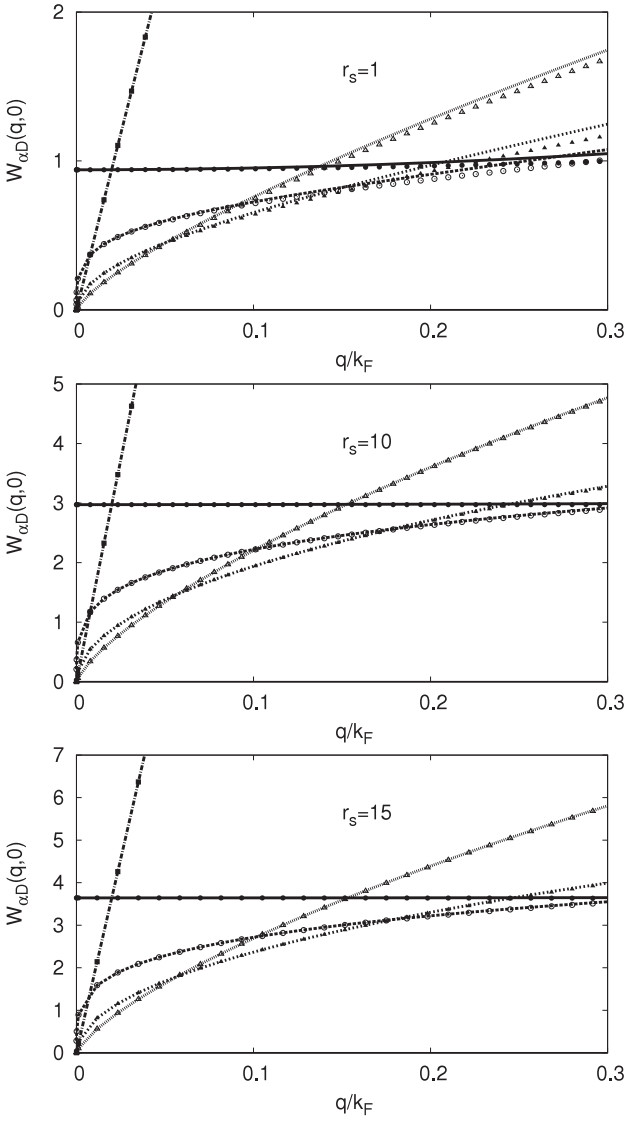

Figure 1. Scaled plasma frequency as a function of plasmon wavevector at zero temperature and $r_s = 1$, 10 and 15. Plasma frequencies calculated in the exact method are compared with those estimated in the plasmon-pole approximation method. In the exact method: solid line ($\alpha = 3$), dashed line ($\alpha = 2.5$), short-dashed line ($\alpha = 2$), dotted line ($\alpha = 1.5$) and dotted–dashed line ($\alpha = 1.01$). In the PPA method: closed circles ($\alpha = 3$), open circles ($\alpha = 2.5$), closed triangles ($\alpha = 2$), open triangles ($\alpha = 1.5$) and closed squares ($\alpha = 1.01$).

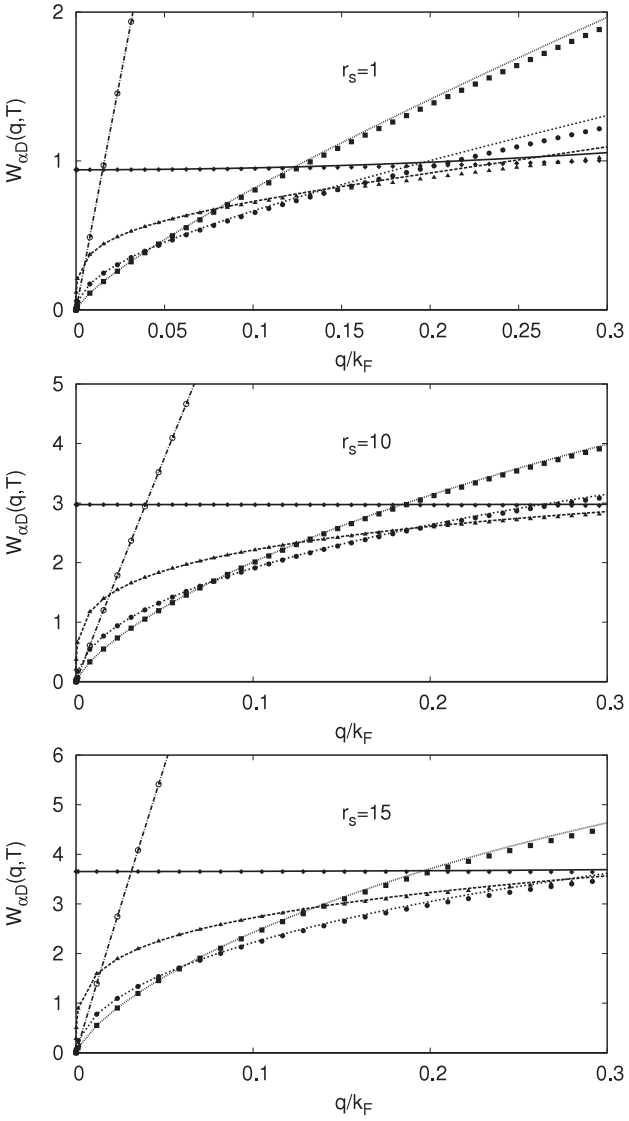

Figure 2. Plasma frequency as a function of wavevector at $T = 0.5T_F$. Notations are the same as in figure 1.

The plasma frequency at temperature T is obtained as

$$\Omega_{\alpha D}(q,T) = \omega_{\alpha D}(q,T) + \frac{q^2 v_\mu^2}{\omega_{\alpha D}^2(q,T)}\left(\frac{3}{2(\alpha+2)} \times \left\{1 + \frac{5\alpha(\alpha+2)\pi^2 k_B^2 T^2}{24\mu^2}\right\} - \frac{\omega_{\alpha D}^2(q,T)\xi_{\alpha D}(T)}{q^2 v_\mu^2}\right) \quad (31)$$

where

$$\xi_{\alpha D}(T) = \frac{(7-\alpha)\Gamma(\frac{\alpha}{2})}{4(\alpha+2)\pi^{\frac{1}{2}}\Gamma(\frac{\alpha+3}{2})}\int_0^\infty [1 - S_{\alpha D}(\mathbf{k};\mu,T)]\,\mathrm{d}k.$$

Unfortunately $\xi_{\alpha D}(T)$ cannot be evaluated analytically. Following the method of Maldague [61], we have got $S_{\alpha D}(\mathbf{k};\mu,T)$ in the numerical method.

The PPA method finds $\Omega_{\alpha D}^{(p)}(q,T)$ as

$$\Omega_{\alpha D}^{(p)}(q,T) = \omega_{\alpha D}(q,T) + \frac{q^2 v_\mu^2}{\omega_{\alpha D}^2(q,T)}\left(\frac{1}{2\alpha}\left\{1 + \frac{5\alpha(\alpha+2)\pi^2 k_B^2 T^2}{24\mu^2}\right\} - \frac{\omega_{\alpha D}^2(q,T)\xi_{\alpha D}(T)}{q^2 v_\mu^2}\right). \quad (32)$$

The scaled plasma frequencies $W_{\alpha D}(q,T)$ obtained in the RPA and PPA methods are compared in figure 2. Both the methods find similar plasma frequencies.

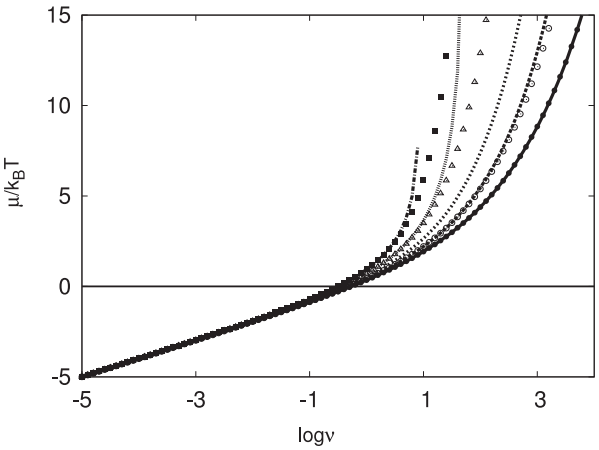

Figure 3. Chemical potentials of the Fermi gas as a function of electron density for several α values. The chemical potentials calculated in the numerical method from equation (A.1) are compared with those obtained in the Padé approximant method equation (A.5). In the exact method: solid line ($\alpha = 3$), dashed line ($\alpha = 2.5$), short-dashed line ($\alpha = 2$), dotted line ($\alpha = 1.5$) and dotted–dashed line ($\alpha = 1.01$). In the Padé approximant method: closed circles ($\alpha = 3$), open circles ($\alpha = 2.5$), open triangles ($\alpha = 1.5$) and closed squares ($\alpha = 1.01$).

Since in the long-wavelength limit $\mathrm{Im}[Q^{(0)}(q, \Omega_{\alpha D}(q, T); \mu, T)] = 0$, the collisionless plasma damping $\gamma_{\alpha D}(q, T)$ vanishes. Thus, the quantum plasma, whether at zero- or finite-temperature below T_F, is undamped in the long-wavelength limit.

5. Long-wavelength plasma frequency and plasma damping in classical plasma

When the temperature is high, the $n_\mathrm{F}(\mathbf{k})$ is described by the Maxwell–Boltzmann distribution function [25]:

$$n_\mathrm{F}(\mathbf{k}) = \sum_{l=1}(-1)^{l-1} \exp\left(\frac{1\mu}{k_\mathrm{B}T}\right) \exp\left(\frac{-1E_k}{k_\mathrm{B}T}\right). \tag{33}$$

The chemical potential μ for $\alpha = 2$ has been derived as [27]

$$\mu = k_\mathrm{B}T \log\left[\exp\left(\frac{\hbar^2\pi n_{2D}}{m^* k_\mathrm{B}T}\right) - 1\right]. \tag{34}$$

For $\alpha \neq 2$, the evaluation of μ is shown in appendix A. It is given as

$$\mu = k_\mathrm{B}T[\log\nu + K_1 \log(K_2\nu + 1) + K_3], \tag{35}$$

where the scaled density $\nu = n_{\alpha D}/n_{\alpha D}^{(0)}$, $n_{\alpha D}^{(0)} = 2/\lambda_T^\alpha$ and the thermal wavelength $\lambda_T = \sqrt{2\pi\hbar^2/m^* k_\mathrm{B}T}$. The method of finding α-dependent constants K_1, K_2 and K_3 are given in appendix A. The chemical potential as a function of ν is shown in figure 3. In the low density regime μ is negative and it is positive when the density is high.

Taking the leading-order term in equation (33), substituting in (6) and carrying out the integration over k, we find

$$\mathrm{Re}[Q_{\alpha D}^0(q, \omega; \mu, T)] = \frac{\omega_{\alpha D}^2(q)}{\omega^2}\left(1 + \frac{3q^2 k_\mathrm{B}T}{m^*\omega^2}\right) + \left(\frac{1}{\omega^6}\right). \tag{36}$$

Using equation (33) in (7), we find

$$\mathrm{Im}[Q^{(0)}(q, \omega; \mu, T)] = -n_{\alpha D}\left(\frac{2\pi m^*}{\hbar^2 k_\mathrm{B}T}\right)^{\frac{1}{2}} \frac{1}{q} \times \exp\left(-\frac{\hbar^2 q^2}{8m^* k_\mathrm{B}T}\right) \exp\left(-\frac{m^*\omega^2}{2q^2 k_\mathrm{B}T}\right) \sinh\left(\frac{\hbar\omega}{2k_\mathrm{B}T}\right). \tag{37}$$

The HF structure factor is thus obtained as

$$S_{\alpha D}^{\mathrm{HF}}(\mathbf{k}) = 1. \tag{38}$$

Therefore $G_{\alpha D}^{\mathrm{HF}}(q, \omega; \mu, T) = 0$ which shows that the contribution of the first-order perturbative contributions due to self-energy and exchange terms to the LFF vanishes. Since the particles are assumed point-like due to their short de Broglie wavelengths, the higher-order many-body corrections do not contribute to the classical plasma frequency.

The plasma frequency is calculated as

$$\Omega_{\alpha D}(q, T) = \omega_{\alpha D}(q)\left[1 + \frac{3}{2}\left(\frac{q}{q_D}\right)^{\alpha-1}\right] \tag{39}$$

where the Debye–Hückel wavevector q_D is defined as

$$q_D^{\alpha-1} = \frac{m^*\omega_{\alpha D}^2(q) q^{\alpha-3}}{k_\mathrm{B}T}. \tag{40}$$

In the PPA method, $\epsilon(q, T) = \epsilon_b[1 + (q/q_D)^{\alpha-1}]$. Using equation (16), the plasma frequency is obtained and it is the same as in equation (39). The classical plasma frequencies are the same in both RPA and PPA methods. These are shown in figure 4 for several α and r_s values.

Since the dynamical LFF vanishes in classical plasma, the plasma damping in the high-temperature limit ($\hbar\omega_{\alpha D}(q)/k_\mathrm{B}T \ll 1$) is obtained as

$$\gamma_{\alpha D}(q, T) = \omega_{\alpha D}(q)\left(\frac{\pi}{8}\right)^{\frac{1}{2}} \frac{q_D^{\frac{3\alpha-3}{2}}}{q^{\frac{\alpha+3}{2}}} \exp\left[-\frac{1}{2}\left(\frac{q_D}{q}\right)^{\alpha-1}\right]. \tag{41}$$

The temperature affects both the damping and $q^{\alpha-1}$ correction to the plasma frequency, but does not alter the leading term. The plasma dampings for several α and r_s values are shown in figure 5. The long-wavelength classical plasma oscillations undergo Landau damping [59] except when $\alpha = 1.01$.

6. Conclusion

In the present work, the plasma frequencies of the quantum and classical plasmas in the long-wavelength limit are derived in the FD space for the first time. Both the modified RPA and PPA methods are used to find plasma frequencies and both methods find similar results. The dynamical LFF, which is a higher-order many-body correction to the plasma frequency, is found to vanish in classical plasma due to a small de Broglie wavelength. The plasma frequency has a gap in the 3D system and it is gapless in all confined systems. Unlike the quantum plasma, the classical plasma is Landau-damped. As mentioned earlier, the determination of α in QWs and quantum wires

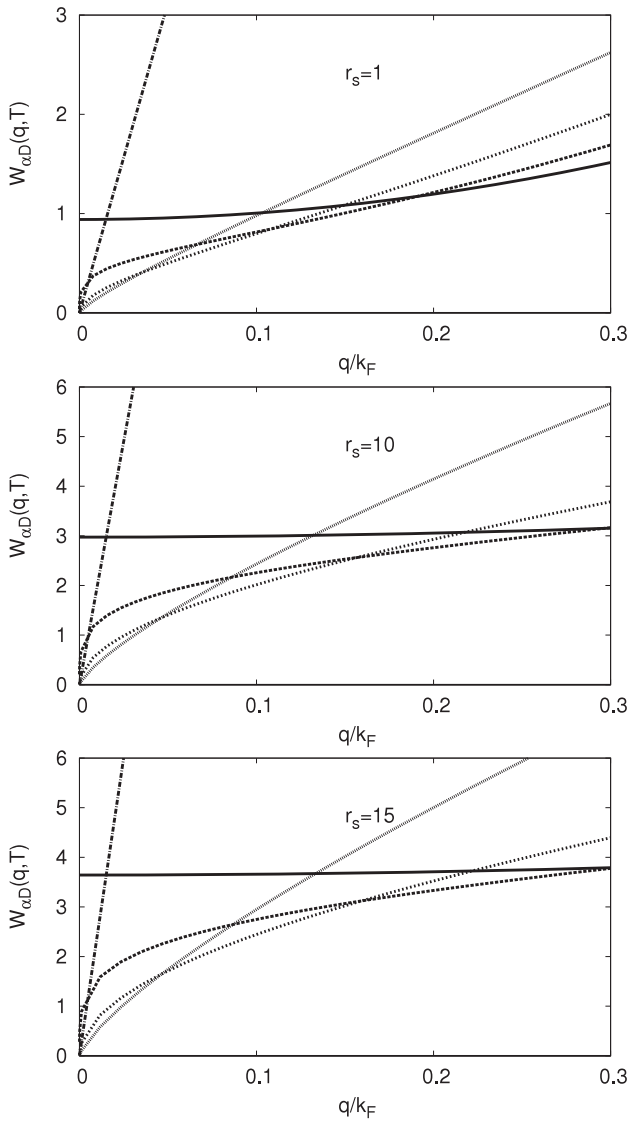

Figure 4. Classical plasma frequency as a function of wavevector at $T = 2T_F$. Notations are the same as in figure 1.

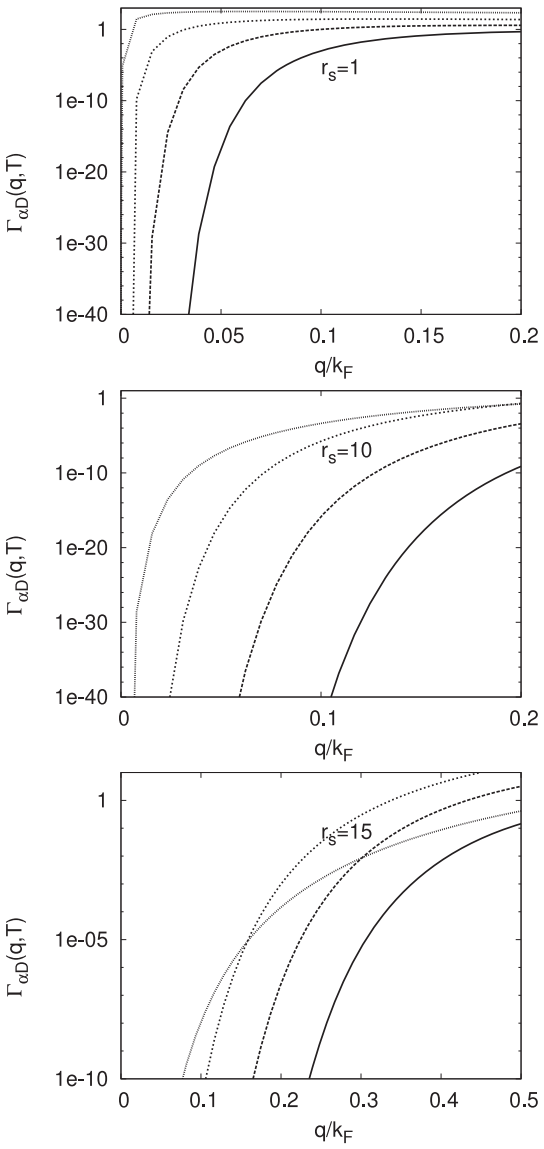

Figure 5. Classical plasma damping as a function of the plasma wavevector for $r_s = 1$, 10 and 15. The damping vanishes at $\alpha = 1.01$. Notations are the same as in figure 1.

depends on the excitation dynamics. In a QW, it is calculated as $\alpha = 3 - \exp(-L/R)$ where L is the well width and R is the radius of exciton and polaron [9, 19]. In the plasmon studies, the radius of the plasmon can be taken to find α.

Acknowledgment

One of the authors (SP) acknowledges the financial support of the Council of Scientific and Industrial Research (CSIR) project 13(8040-A)/Pool/2005 to carry out this work.

Appendix. Chemical potential

The number of electrons is defined as $N_{\alpha D} = 2\sum_k n_F(k)$. Using equation (9) the electron density is obtained as

$$n_{\alpha D} = n^0_{\alpha D} \sum_{L=1}^{\infty} (-1)^{l-1} \frac{1}{L^{1/2}} \exp\left(l \frac{\mu}{k_B T}\right) \tag{A.1}$$

The chemical potential can be obtained from equation (A.1) in the zero-finding method. However, we have presented an analytic method for finding it. Following the method of Joyce–Dixon [62], the chemical potential is expressed as

$$\frac{\mu}{k_B T} = \log \nu + \sum_{n=1} B_n \nu^n \tag{A.2}$$

where $B_1 = 1/2^{\alpha/2}$, $B_2 = 3/2^{\alpha+1} - 1/3^{\alpha/2}$, $B_3 = 1/2^{\alpha} + (10/3)/2^{3\alpha/2} - 4/6^{\alpha/2}$, etc. The logarithmic derivative of equation (A.2) gives

$$\nu \frac{\mathrm{d}}{\mathrm{d}\mu}\left(\frac{\mu}{k_B T}\right) = 1 + \sum_{n=1}^{\infty} n B_n \nu^n. \tag{A.3}$$

The right-hand side (rhs) of this equation is expressed in terms of the $\{L/M\}$ Padé approximant form [63]. We find that the $\{2/1\}$ Padé approximant form gives the best fit for all α. In this

form the rhs of equation (A.3) is expressed as

$$1 + \sum_n n B_n \nu^n = \frac{1 + p_1\nu + p_2\nu^2}{1 + q_1\nu} \tag{A.4}$$

where p_1, p_2 and q_1 are the coefficients. These coefficients are obtained as $q_1 = -3B_3/2B_2$, $p_1 = B_1 - q_1$ and $p_2 = 2B_2 - B_1 p_1$. In the {2/1} Padé approximant method, only B_1, B_2 and B_3 are sufficient to find q_1, p_1 and p_2. Finally the integration yields [27, 64]

$$\mu = k_B T[\log \nu + K_1 \log(K_2\nu + 1) + K_3\nu \tag{A.5}$$

where $K_1 = (p_1q_1 - p_2 - q_1^3)/q_1^2$, $K_2 = q_1$ and $K_3 = p_2/q_1$.

References

[1] Mathieu H, Lefebvre P and Christol P 1992 *J. Appl. Phys.* **72** 300
[2] Singh J and Thilagam A 1994 *Phys. Rev.* B **49** 13583
[3] Harrison P 2000 *Quantum Wells, Wires and Dots* (New York: Wiley)
[4] Smondyrev M A, Gerlach B and Dzero M O 2000 *Phys. Rev.* B **62** 16692
[5] Hai G Q, Peeters F M and Devreese J T 1998 *Phys. Rev.* B **48** 4666
[6] Stillinger F H 1977 *J. Math. Phys.* **18** 1224
[7] He X-F 1987 *Solid State Commun.* **61** 53
[8] He X-F 1991 *Phys. Rev.* B **43** 2063
[9] Lefebvre P, Christol P, Mathieu H and Glutsch S 1995 *Phys. Rev.* B **52** 5756
[10] Karlsson K F, Dupertuis M-A, Weman H and Kapon E 2006 *Phys. Rev.* B **70** 153306
[11] Thilagam A 1997 *Phys. Rev.* B **55** 7804
[12] Mizeikis V, Birkedal D, Langebein W, Lyssenko V G and Hvam J M 1997 *Phys. Rev.* B **55** 5284
[13] Mizeikis V, Singh J, Lyssenko V G, Erland J and Hvam J M 1997 *Phys. Rev.* B **55** 5284
[14] Thilagam A 1997 *Phys. Rev.* B **56** 9798
[15] Thilagam A 1997 *Phys. Rev.* B **56** 4665
[16] Tanguy C, Lefebvre P, Mathieu H and Elliot R J 1997 *J. Appl. Phys.* **82** 798
[17] Reyes-Gomez E, Matos-Abiague A, Perdomo-Leiva C A, de Dios-Leyva M and Oliveira L E 2000 *Phys. Rev.* B **61** 13104
[18] Thilagam A 1999 *Phys. Rev.* B **59** 3027
[19] Matos-Abiague A 2002 *J. Phys.: Condens. Matter* **14** 4543
[20] Matos-Abiague A 2002 *Phys. Rev.* B **65** 165321
[21] Thilagam A and Matos-Abiague A 2004 *J. Phys.: Condens. Matter* **16** 3981
[22] Rohlfing M and Louie S G 1998 *Phys. Rev. Lett.* **81** 2312
[23] Ping C-Y and Chuang S L 1993 *Phys. Rev.* B **48** 8210
[24] Tempere J and Devreese J T 2001 *Phys. Rev.* B **64** 104504
[25] Fetter A L and Walecka J D 1971 *Quantum Theory of Many-Particle System* (New York: McGraw-Hill)
[26] Mahan G D 2000 *Many-Particle Physics* (New York: Plenum)
[27] Haug H and Koch S W 2000 *Quantum Theory of the Optical Properties of Semiconductors* (Singapore: World Scientific)
[28] Giuliani G F and Vignale G 2005 *Quantum Theory of the Electron Liquid* (Cambridge: Cambridge University Press)
[29] Fleszar A and Resta R 1985 *Phys. Rev.* B **31** 5305
[30] Das Sarma S and Hwang E H 1996 *Phys. Rev.* B **54** 1936
[31] Lundqvist B I 1967 *Phys. Kondens. Matter* **6** 193
[32] Wendler L and Pechstedt R 1986 *Phys. Status Solidi* b **138** 197
[33] Das Sarma S, Hwang E H and Zheng L 1996 *Phys. Rev.* B **54** 8057
[34] Pinsook J and Sa-Yakanit V 2003 *Phys. Status Solidi* b **237** 82
[35] Das Sarma S, Jain J K and Jalabert J 1988 *Phys. Rev.* B **37** 4560
[36] Simion G E and Giuliani G F 2008 *Phys. Rev.* B **77** 035131
[37] Lindhard J 1954 *K. Danske Vidensk. Selsk. Mat.-Fys. Meddr.* **28** 8
[38] Stern F 1967 *Phys. Rev. Lett.* **18** 546
[39] Zhang Y and Das Sarma S 2004 *Phys. Rev.* B **70** 035104
[40] Hwang E H and Das Sarma S 2001 *Phys. Rev.* B **64** 165409
[41] Sturm K and Gusarov A 2000 *Phys. Rev.* B **62** 16474
[42] Holas A, Arabind P K and Singwi K S 1979 *Phys. Rev.* B **20** 4912
[43] Czechor A, Holas A, Sarma S and Singwi K S 1986 *Phys. Rev.* B **25** 2144
[44] Atwal G S, Khalil I G and Ashcroft N W 2003 *Phys. Rev.* B **67** 115107
[45] Tanatar B and Damirel E 2000 *Phys. Rev.* B **62** 1787
[46] Calmels L and Gold A 1995 *Phys. Rev.* B **52** 10841
[47] Lowe D and Barker J R 1985 *J. Phys. C: Solid State Phys.* **18** 2507
[48] Rorison J M and Herbert D C 1986 *J. Phys. C: Solid State Phys.* **19** 3991
[49] Fetter A L 1974 *Phys. Rev.* B **10** 3739
[50] Beck D E and Kumar P 1976 *Phys. Rev.* B **13** 2859
[51] Platzman P M and Tzoar N 1976 *Phys. Rev.* B **13** 3197
[52] Studart N and Hipolito O 1979 *Phys. Rev.* A **19** 1790
[53] Studart N and Hipolito O 1980 *Phys. Rev.* A **22** 2860
[54] Hubbard J 1957 *Proc. R. Soc.* A **243** 336
[55] Abramowitz M and Stegun I 1970 *Handbook of Mathematical Functions* (New York: Dover)
[56] Thakur J S and Pathak K N 1983 *J. Phys. C: Solid State Phys.* **16** 6551
[57] Bares P-A and Wen X-G 1993 *Phys. Rev.* B **48** 8636
[58] Bartosch L and Kopietz P 1999 *Phys. Rev.* B **59** 5377
[59] Landau L D 1946 *J. Phys. (USSR)* **10** 25
[60] Cetina E, Magana F and Valladares A A 1977 *Am. J. Phys.* **45** 960
[61] Maldague P F 1978 *Surf. Sci.* **73** 296
[62] Joyce W B and Dixon R W 1977 *Appl. Phys. Lett.* **31** 354
[63] Baker G A 1981 Pade approximation *Encyclopedia of Mathematics and its Applications* (Reading, MA: Addison-Wesley) part 1
[64] Aguilera-Navarvo G A, Estevez G A and Kostecki A 1988 *J. Appl. Phys.* **63** 2843